

**FINAL REPORT**  
**OTKA/NKFIH 138930 PD project**

**TARGETED MULTIARMED POLYPEPTIDE NANOCARRIERS FOR DRUG  
DELIVERY ACROSS THE BLOOD-BRAIN BARRIER**

---

**Papers with acknowledgement of the OTKA/NKFIH 138930 PD project**

1. **Mészáros M**, Phan THM, Vigh JP, Porkoláb G, Kocsis A, Szecskó A, Páli EK, Cser NM, Polgár TF, Kecskeméti G, Walter FR, Schwamborn JC, Janáky T, Jan JS, Veszelka S, Deli MA. Alanine and glutathione targeting of dopamine- or ibuprofen-coupled polypeptide nanocarriers increases both crossing and protective effects on a blood-brain barrier model. *Fluids Barriers CNS*. 2025;22(1):18. doi: 10.1186/s12987-025-00623-2. **IF: 5.9, D1.**
2. Szecskó A\*, **Mészáros M\***, Simões B\*, Cavaco M, Chaparro C, Porkoláb G, Castanho MARB, Deli MA, Neves V, Veszelka S. PepH3-modified nanocarriers for delivery of therapeutics across the blood-brain barrier. *Fluids Barriers CNS*. 2025 Apr 1;22(1):31. doi: 10.1186/s12987-025-00641-0. PMID: 40170024; PMCID: PMC11959756. **IF: 5.9, D1.**
3. Kecskés S\*, **Mészáros M\***, Dvorácskó S\*, Szabó Í, Porkoláb G, Barna L, Harazin A, Szecskó A, Menyhárt Á, Bari F, Deli MA, Penke B, Farkas E, Veszelka S. The impact of the novel  $\sigma_1$  receptor ligand (S)-L1 on brain endothelial cells and cerebrovascular reactivity challenged by ischemia. *Eur J Pharmacol*. 2025;1000:177724. doi: 10.1016/j.ejphar.2025.177724. **IF: 4.2, Q1.**
4. Porkoláb G, **Mészáros M**, Szecskó A, Vigh JP, Walter FR, Figueiredo R, Kálomista I, Hoyk Z, Vizsnyiczai G, Gróf I, Jan JS, Gosselet F, Purity MK, Vastag M, Hudson N, Campbell M, Veszelka S, Deli MA. Synergistic induction of blood-brain barrier properties. *Proc Natl Acad Sci U S A*. 2024;121(21):e2316006121. doi: 10.1073/pnas.2316006121. **IF: 9.4, D1.**
5. Deli MA, Porkoláb G, Kincses A, **Mészáros M**, Szecskó A, Kocsis AE, Vigh JP, Valkai S, Veszelka S, Walter FR, Dér A. Lab-on-a-chip models of the blood-brain barrier: evolution, problems, perspectives. *Lab Chip*. 2024;24(5):1030-1063. doi: 10.1039/d3lc00996c. **IF: 6.1, Q1.**
6. **Mészáros M**, Phan THM, Vigh JP, Porkoláb G, Kocsis A, Páli EK, Polgár TF, Walter FR, Bolognin S, Schwamborn JC, Jan JS, Deli MA, Veszelka S. Targeting Human Endothelial Cells with Glutathione and Alanine Increases the Crossing of a Polypeptide Nanocarrier through a Blood-Brain Barrier Model and Entry to Human Brain Organoids. *Cells*. 2023;12(3):503. doi: 10.3390/cells12030503. **IF: 7.7, Q1.**
7. Veszelka S\*, **Mészáros M\***, Porkoláb G, Rusznyák Á, Réti-Nagy KS, Deli MA, Vecsernyés M, Bácskay I, Váradi J, Fenyvesi F. Effects of Hydroxypropyl-Beta-Cyclodextrin on Cultured Brain Endothelial Cells. *Molecules*. 2022 Nov 10;27(22):7738. doi: 10.3390/molecules27227738. **IF: 4.9, Q1.**

8. Lee MH, Jan JS, Thomas JL, Shih YP, Li JA, Lin CY, Ooya T, Barna L, **Mészáros M**, Harazin A, Porkoláb G, Veszelka S, Deli MA, Lin HY. Cellular Therapy Using Epitope-Imprinted Composite Nanoparticles to Remove  $\alpha$ -Synuclein from an In Vitro Model. *Cells*. 2022;11(16):2584. doi: 10.3390/cells11162584. **IF: 7.7, Q1.**
  
9. Kokhanyuk B, Vántus VB, Radnai B, Vámos E, Kajner G, Galbács G, Telek E, **Mészáros M**, Deli MA, Németh P, Engelmann P. Distinct Uptake Routes Participate in Silver Nanoparticle Engulfment by Earthworm and Human Immune Cells. *Nanomaterials (Basel)*. 2022;12(16):2818. doi: 10.3390/nano12162818. PMID: 36014683; PMCID: PMC9413649. **IF: 4.9, Q1.**
  
10. Akel H, Csóka I, Ambrus R, Bocsik A, Gróf I, **Mészáros M**, Szecskó A, Kozma G, Veszelka S, Deli MA, Kónya Z, Katona G. In Vitro Comparative Study of Solid Lipid and PLGA Nanoparticles Designed to Facilitate Nose-to-Brain Delivery of Insulin. *Int J Mol Sci*. 2021;22(24):13258. doi: 10.3390/ijms222413258. **IF: 5.5, D1.**
  
11. Veszelka S\*, **Mészáros M\***, Porkoláb G\*, Szecskó A, Kondor N, Ferenc G, Polgár TF, Katona G, Kóta Z, Kelemen L, Páli T, Vigh JP, Walter FR, Bolognin S, Schwamborn JC, Jan JS, Deli MA. A Triple Combination of Targeting Ligands Increases the Penetration of Nanoparticles across a Blood-Brain Barrier Culture Model. *Pharmaceutics*. 2021;14(1):86. doi: 10.3390/pharmaceutics14010086. PMID: 35056983; PMCID: PMC8778049. **IF: 6.1, Q1.**

\*These authors contributed equally to this work.

Six first author papers and five co-author manuscript related to the project were published (**total IF: 68.3**).

## Introduction

The pharmaceutical treatment of central nervous system (CNS) disorders, like neurodegenerative diseases, is far from satisfactory due to the poor penetration of drugs to the brain tissue (Neuwelt et al., 2008). The blood-brain barrier (BBB) is the major obstacle to prevent potential neuropharmaceuticals to reach their targets (Pardridge, 2017). Several clinical trials ended with failure because of the low penetration of biological drugs across the BBB (Pardridge, 2016). Nanocarriers can increase brain delivery of therapeutics, but specific targeting is needed to cross the BBB (Kreuter, 2014; Mc Carthy et al., 2015). We described targeting vectors of nutrient transporters to increase the transfer of NPs with model molecule cargo across BBB in culture models and in mice (Veszeka et al., 2017; Mészáros et al., 2018). Gold standard BBB culture models are based on primary brain endothelial cells isolated from animal tissues (Veszeka et al., 2018). Due to species differences at BBB transporter levels (Uchida et al., 2020) the development of human cell-based models has high importance, but barrier or endothelial properties of current human stem cell derived models are problematic.

Our aim (1) was to improve a human BBB co-culture system established in our laboratory for testing drug delivery approaches. Based on our published results alanine and glutathione targeting ligands increase the BBB permeability of nanoparticles. Therefore, aim (2) was a proof-of-concept study with these targeting ligands to provide elevated permeability across the human BBB model for a novel multiarmed polypeptide nanocarrier coupled with active agents, namely ibuprofen and dopamine, which have low brain penetration. We also investigated the protective effects of targeted ibuprofen-loaded nanocarriers against cytokine-induced damage on the cells of the neurovascular unit. The entry of dopamine-coupled nanocarriers into midbrain organoids derived from healthy or Parkinson's disease patients was also studied both static and microfluidic human BBB models. Aim (3) was to investigate the cellular uptake mechanisms and the intracellular fate of the targeted polypeptides.

## Results

### 1. HUMAN BLOOD-BRAIN BARRIER MODEL DEVELOPMENT

The first main goal was to develop an improved and physiologically more relevant human blood-brain barrier (BBB) model based on the co-culture of vascular endothelial cells derived from human cord blood stem cells with brain pericytes using novel small molecular differentiation factors. To enhance BBB properties, we activated the cyclic AMP/PKA and Wnt/ $\beta$ -catenin signaling pathways, and inhibited the TGF- $\beta$  pathway. (**Fig.1A**). To target this interaction, we presented a small-molecule cocktail named cARLA, which synergistically enhances barrier tightness in a range of BBB models (**Fig.1B; Porkoláb et al., 2024**).

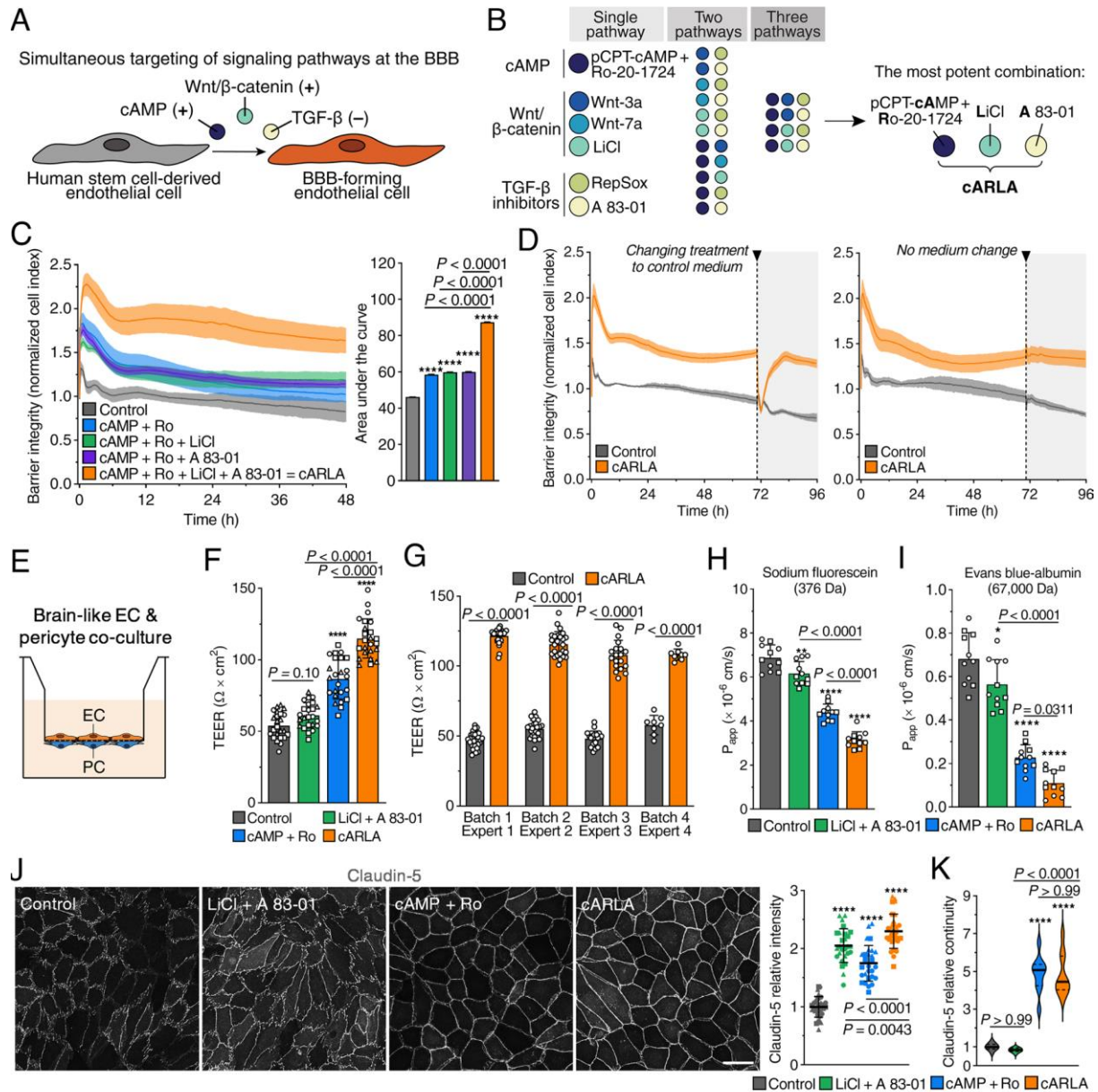


**Fig. 1.** cARLA synergistically enhances barrier tightness via claudin-5. (A) Rationale. (B) Schematic drawing of single compounds and their combinations tested in the impedance-based screen. (C) Barrier integrity of human cord blood stem cell-derived EC monolayers supplemented with PC-conditioned medium, measured by impedance. Higher normalized cell index values and a higher area under the curve indicate increased barrier integrity. Mean  $\pm$  SD, ANOVA with Bonferroni's post hoc test, \*\*\*\* $P < 0.0001$  compared to the control group,  $n = 6$ . (D) Impedance kinetics of EC monolayers with or without changing cARLA treatment to control medium at 72 h. Mean  $\pm$  SD,  $n = 6$ . (E) Schematic drawing of the BBB model: human stem cell-derived ECs acquire brain-like characteristics upon coculture with PCs. (F) Transendothelial electrical resistance (TEER) in the coculture model after 48 h treatment. Mean  $\pm$  SD, ANOVA with Bonferroni's post hoc test, \*\*\*\* $P < 0.0001$  compared to the control group,  $n = 24$  from three experiments. (G) Reproducibility of TEER measurements after 48 h cARLA treatment across experiments, measured by different experts using different batches of cells. Mean  $\pm$  SD, ANOVA with Bonferroni's post hoc test,  $n = 82$  from four experiments. (H) Permeability of sodium fluorescein and (I) Evans blue-albumin across the coculture model after 48 h treatment.  $P_{app}$ : apparent permeability coefficient. Mean  $\pm$  SD, ANOVA with Bonferroni's post hoc test, \* $P < 0.05$ , \*\* $P < 0.01$ , \*\*\*\* $P < 0.0001$  compared

to the control group,  $n = 11$  from two experiments. (J) Claudin-5 immunostaining in human brain-like ECs. (Scale bar:  $50\ \mu\text{m}$ .) Mean  $\pm$  SD for intensity and (K) median  $\pm$  quartiles for continuity, ANOVA with Bonferroni's post hoc test, \*\*\*\* $P < 0.0001$  compared to the control group,  $n = 27$  to  $30$  from three experiments (Porkoláb et al., 2024).

#### *Characterization of the model – impedance kinetics*

To find the optimal concentrations and combinations of small molecules (LiCl, RepSox, A83-01) and recombinant proteins (Wnt-3a, Wnt-7a) we performed real-time impedance-based (RTCA-SP, ACEA Biosciences) assay to measure effects on barrier tightness in cultured human vascular endothelial cell layers receiving brain pericyte-conditioned medium. We optimized the treatment durations and concentrations of pathway inducers alone and in multiple combinations. We observed that the Wnt activation together with TGF- $\beta$  inhibition increases barrier integrity compared to targeting single pathways (Fig.1C; Porkoláb et al., 2024). We identified a potent combination of small molecules targeting these three pathways which greatly and synergistically elevated the impedance of human endothelial cell layers in a long-lasting ( $>72$  h) manner (Fig.1D; Porkoláb et al., 2024).

#### *Measurements of transendothelial electrical resistance*

We also measured the effects of the optimized combination of molecules in a BBB model in which human vascular endothelial cells were co-cultured with brain pericytes. Transendothelial electrical resistance was synergistically increased (2-fold compared to the non-treated group) by the identified best signaling pathway targeting combination. (Fig.1E-G; Porkoláb et al., 2024).

#### *Permeability of marker molecules*

We measured lower permeability for tracers sodium fluorescein (50% decrease) and Evans blue-albumin (80% decrease compared to the control group) across the co-culture model, indicating that the small molecule combination tightened both the para- and transcellular pathways BBB (Fig.1H-I; Porkoláb et al., 2024).

#### *Fluorescent microscopy of BBB specific junctional protein*

The small molecule combination elevated both the staining intensity (2-fold) and the continuity (5-fold) of the tight junction protein claudin-5 at the cell borders investigated by immunocytochemistry and fluorescent microscopy (Fig.1J-K; Porkoláb et al., 2024).

#### *Gene expression of selected endothelial and BBB marker proteins and transporters*

To investigate gene expressional changes in brain-like endothelial cells upon the best BBB-inducing treatment Massive Analysis of cDNA Ends (MACE) sequencing of the collected mRNA samples was performed GenXPro, Frankfurt, Germany) (Fig.2A-B; Porkoláb et al., 2024). In the treatment group 619 genes were upregulated and 546 downregulated (Fig.2C). We observed the key genes related to BBB functions were upregulated by the molecular combination, including genes encoding the efflux pump P-glycoprotein/ABCB1, the glucose transporter-1 and claudin-5 junctional protein. On a pathway level, an overrepresentation of genes related to endothelial cells differentiation and barrier formation as well as maturation and quiescence was found. This was also accompanied by a marked redistribution of F-actin from stress fibers and focal adhesions to the cortical actin cytoskeleton, supporting the maturation of

cell-cell contacts (visualized by actin staining and confocal microscopy) (Porkoláb et al., 2024).

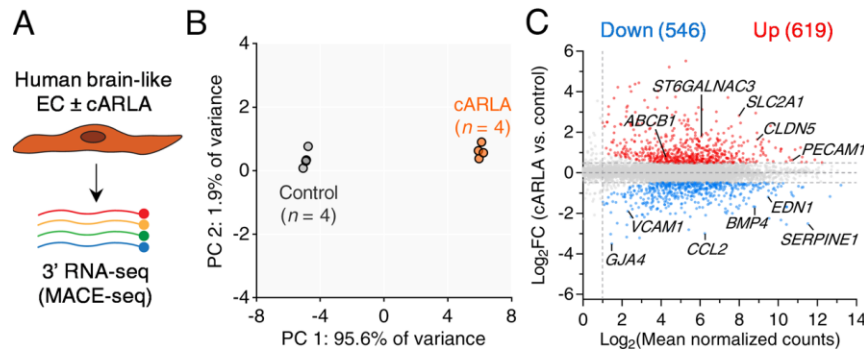


**Fig. 2.** *cARLA promotes barrier maturation and brain endothelial identity in human brain-like endothelial cells (ECs).* (A) Schematic drawing of the experimental setup. (B) Principal component analysis (PCA) of control and cARLA-treated samples. (C) Mean-difference (MD) plot of cARLA vs. control samples showing up-and down-regulated genes and their expression levels. Key transcripts related to different aspects of BBB function are highlighted (Porkoláb et al., 2024).

The MACE-seq profiling revealed that the small molecule combination can influence several aspects of BBB maturation in addition to junctional tightness. To explore the ability of the molecular combination to induce a complex BBB phenotype, we validated findings at the protein and functional level for selected BBB properties in brain-like human endothelial cells (Porkoláb et al., 2024). Efflux pump activity was measured by the bidirectional [blood-to-brain (A-B) and brain-to-blood (B-A)] permeability of rhodamine 123, a ligand of ABCB1 and ABCG2 efflux pumps, across the co-culture BBB model. The efflux ratio (B-A/A-B) of rhodamine 123 was 2.1 in the treatment group (a 1.6-fold increase compared to the control group), which could be reduced to a ratio of 1 using verapamil, an efflux pump inhibitor. These data indicate higher activity and appropriate polarity of efflux pumps in brain-like endothelial cells treated with small molecule ligands targeting the BBB signaling pathways (Porkoláb et al., 2024).

Finally, to put cARLA into practice, we assessed the penetration of 10 clinically used small-molecule drugs across the co-culture model, with or without cARLA treatment. As a consequence, the cARLA-treated human BBB model could correctly discriminate between drugs that readily enter the central nervous system in vivo and those that do not (Porkoláb et al., 2024). We also tested the effect of cARLA on the penetration of brain-targeted nanocarriers by assessing the permeability of polypeptide nanoparticles (NPs) decorated with or without the BBB-specific targeting ligand glutathione (GSH). In agreement with lower basal levels of endocytosis upon cARLA treatment, the permeability of non-targeted NPs was lower across the cARLA-treated BBB model compared to the control group (Fig.3G). Notably, the BBB-specific targeting effect of GSH was apparent in the cARLA-treated but not in the control model, based on both the permeability (Fig.3G) and internalization of NPs in ECs (Fig.3H).



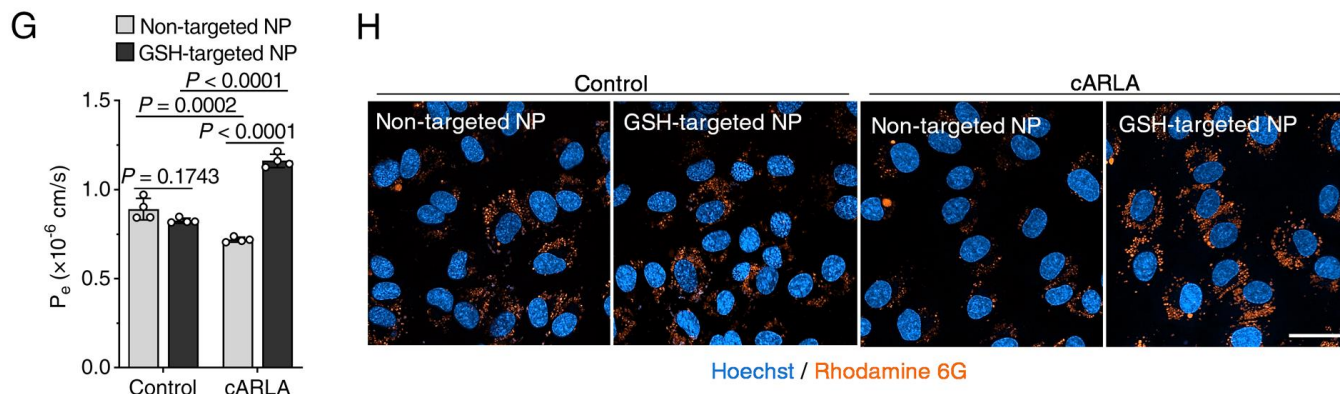


**Fig. 3.** (G) Permeability of nontargeted and GSH-targeted NPs across the coculture BBB model, with or without cARLA treatment.  $P_e$ : endothelial permeability coefficient. Mean  $\pm$  SD, two-way ANOVA with Bonferroni's post hoc test,  $n = 4$ . (H) Internalization of nontargeted and GSH-targeted NPs carrying rhodamine 6G cargo (orange) in ECs, visualized by live cell confocal microscopy. (Scale bar: 50  $\mu\text{m}$ ) (Porkoláb et al., 2024).

Taken together, our results demonstrate that by inducing several aspects of BBB function, cARLA can improve the *in vitro* prediction of therapeutic drug and nanocarrier transport across the human BBB.

The Hungarian (P2300053) and the international (WO2024165877) patenting processes of “Combination of compounds for developing in vitro models of the blood-brain barrier” have been started.

## 2. INVESTIGATION OF TARGETED MULTIARMED POLYPEPTIDE NANOCARRIERS ON AN IMPROVED HUMAN BLOOD-BRAIN BARRIER MODEL

The second main goal of the project was the investigation of **drug-coupled** targeted multiarmed polypeptide nanocarriers on the physiologically more relevant human blood-brain barrier (BBB) model created and characterized by our research group (Porkoláb et al., 2024). The three-armed poly(L-glutamic acid) nanocarriers targeted with alanine and glutathione (3-PLG-A-GSH) were prepared by our collaboration partner Prof. Jeng-Shiung Jan (Department of Chemical Engineering, National Cheng Kung University, Tainan, Taiwan). In Year 1 we characterized the physicochemical properties and explored the internalization and transfer of the 3-PLG-A-GSH nanocarrier without drugs on a human BBB model (Mészáros et al., 2023). In Year 2 the targeted nanocarriers were coupled with two active compounds, the non-steroid anti-inflammatory drug ibuprofen (3-PLG-ibu-A-GSH) and the neurotransmitter dopamine, a key biomolecule in Parkinson's disease (3-PLG-dopa-A-GSH) (Fig.4A; Mészáros et al., 2025).

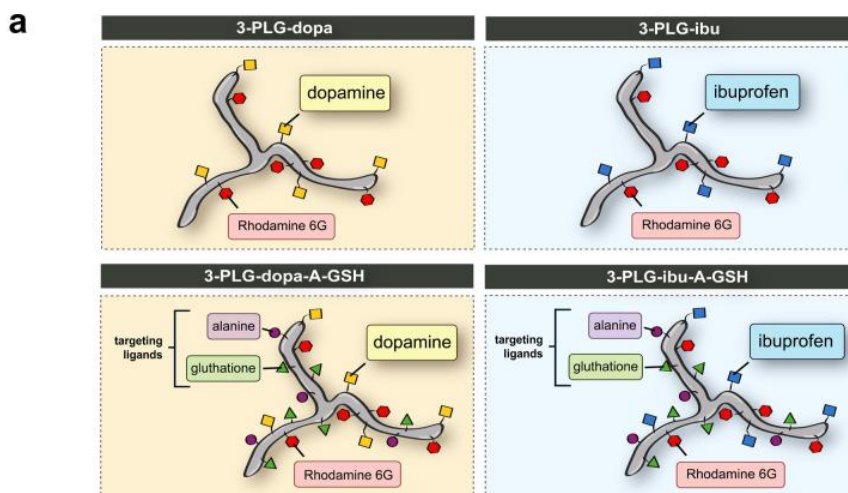


**Fig. 4.** Characterization of nanocarriers. *a* Schematic drawing of non-targeted, 3-armed poly(L-glutamic acid) nanocarriers grafted with dopamine (3-PLG-dopa) or ibuprofen (3-PLG-ibu) and their L-alanine (A) and glutathione (GSH) dual-targeted (3-PLG-dopa-A-GSH; 3-PLG-ibu-A-GSH) formulations. The copolypeptides were labeled by rhodamine 6G (R6G) (Mészáros *et al.*, 2025).

All of the nanocarriers were labeled with the fluorescent dye rhodamine 6G (R6G). These three-armed, drug-coupled nanocarriers were tested on the improved human BBB culture model under physiological and pathological conditions.

#### *Characterization of the targeted drug-coupled polypeptides*

The size, polydispersity index and zeta potential of polypeptide nanocarriers were measured by dynamic light scattering (Malvern Zetasizer Nano ZS). The average hydrodynamic diameter of ibuprofen-coupled nanocarriers was 550 nm for the non-targeted ibuprofen-coupled (3-PLG-ibu) and 330 nm for 3-PLG-ibu-A-GSH (Mészáros *et al.* 2025). The size of dopamine-coupled nanocarriers were around 500 nm (3-PLG-dopa: 520 nm; 3-PLG-dopa-A-GSH: 490 nm). The polydispersity index (PDI) varied between 0.5–0.7 values in all groups, indicating a wider size distribution of the nanocarriers. Size and PDI values of the nanocarriers were in concordance with the images made by transmission electron microscopy (JEOL). All nanocarriers showed filamentous and branched shape in the submicron range. The size and the PDI of nanoparticles did not change significantly until 4 months of storage reflecting the stability of the carriers in solution. The zeta potential of 3-PLGs was highly negative ( $\leq -24$  mV) both in the ibuprofen and in the dopamine-coupled groups that may protect the nanocarriers from aggregation (Mészáros *et al.*, 2025).

#### *Effect of dual-targeted and drug-coupled nanocarriers on the viability of human brain endothelial cells*

The cellular effects of ibuprofen or dopamine coupled 3-PLG and 3-PLG-A-GSH nanocarriers on the improved human endothelial cells were monitored by label-free, real-time impedance measurement in the concentration range of 1–100  $\mu\text{g/ml}$  for 24 h. In this treatment period, we did not detect decrease in the impedance of cell layers reflecting good cell viability and maintenance of the barrier properties. The cell index was not significantly reduced as compared to the control group receiving culture medium only. We concluded that drug-coupled nanocarriers can be used for further experiments at 100  $\mu\text{g/ml}$  or lower concentrations without cell toxicity (Mészáros *et al.* 2025).

#### *Uptake, mechanisms of cellular internalization and the permeability of nanocarriers using the improved human BBB-model under physiological conditions*



Besides the good cytocompatibility, the targeted and drug-coupled nanocarriers (3-PLG-ibu-A-GSH, 3-PLG-dopa-A-GSH) showed elevated time-dependent cellular uptake in human brain endothelial cells (**Fig. 5A-B**). The uptake was quantified by spectrofluorometry measurements (Horiba) and visualized by confocal microscopy (Olympus). Co-treatment with free ligands alanine and glutathione (5mM each) significantly decreased the uptake of targeted nanocarriers (**Fig. 5A-B**). This experiment verified the contribution of targeting ligands in the cellular uptake process.

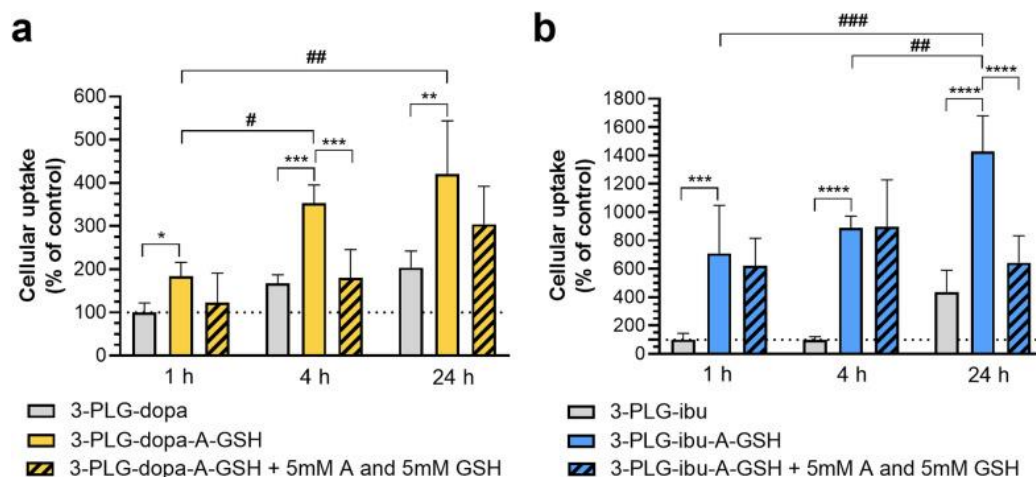


**Fig. 5.** Cellular uptake of *a* dopamine- (3-PLG-dopa; 3-PLG-dopa-A-GSH) or *b* ibuprofen-coupled (3-PLG-ibu; 3-PLG-ibu-A-GSH) nanocarriers in brain endothelial cells after 1, 4 and 24 h of incubation (100  $\mu$ g/ml; 37  $^{\circ}$ C) and the effect of free *l*-alanine and glutathione (GSH) ligands (5 mM each in co-treatment with nanocarriers) on the cellular internalization of dual-targeted nanocarriers. Values presented are means  $\pm$  SD and given as a percentage of the 3-PLG-dopa or 3-PLG-ibu groups at 1 h-time point. Statistical analysis: two-way ANOVA, Tukey's post-test; \* $p$  < 0.05; \*\* $p$  < 0.01; \*\*\* $p$  < 0.001; \*\*\*\* $p$  < 0.0001 compared to the 3-PLG-dopa-A-GSH or 3-PLG-ibu-A-GSH groups at each time-points; # $p$  < 0.05; ## $p$  < 0.01; ### $p$  < 0.001 between the 3-PLG-dopa-A-GSH or 3-PLG-ibu-A-GSH groups at each time point;  $n$  = 6 (Mészáros *et al.*, 2025).

To detect the intracellular fate of the dopamine-(3-PLG-dopa; 3-PLG-dopa-A-GSH) or ibuprofen-coupled (3-PLG-ibu; 3-PLG-ibu-A-GSH) nanocarriers we performed co-localization imaging with the Golgi apparatus in living brain endothelial cells (Mészáros *et al.* 2025). Nanocarriers, especially the targeted ones, could be visualized in the cytoplasm of cells but not in Golgi. Based on image analysis, the co-localization area of Golgi and nanocarriers was limited. The endocytosis inhibitors randomly methylated  $\beta$ -cyclodextrin and cytochalasin D reduced the uptake of dopamine- (3-PLG-dopa-A-GSH) or ibuprofen- coupled (3-PLG-ibu; 3-PLG-ibu-A-GSH) nanocarriers (**Fig. 6A-B**; Mészáros *et al.*, 2025). Both inhibitors decreased the cellular internalization of targeted nanoparticles to less than half as compared to the baseline levels of the control groups. These data indicate that the uptake mechanism of nanocarriers was mediated by endocytosis. The metabolic inhibitor sodium azide also significantly reduced the cellular uptake of the nanocarriers, suggesting an active cellular process (Mészáros *et al.*, 2025).

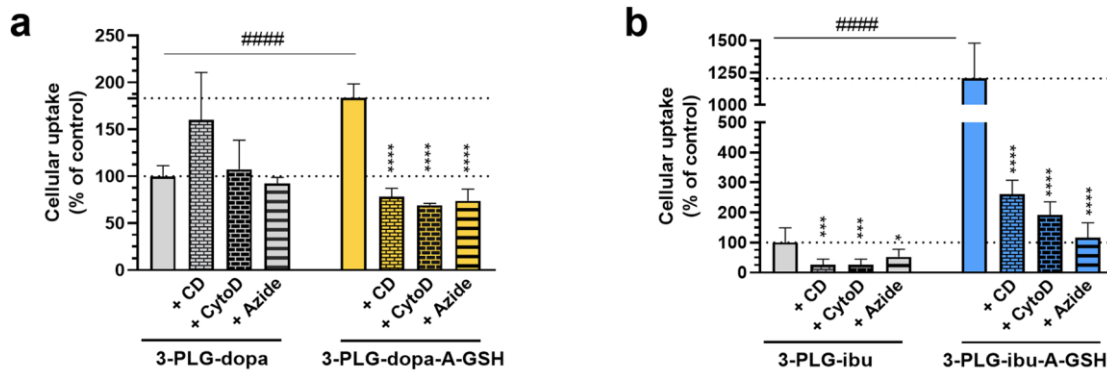


**Fig. 6.** Mechanisms of nanocarrier cell entry. The effects of endocytosis inhibitors randomly methylated  $\beta$ -cyclodextrin (CD) or cytochalasin D (CytoD) and metabolic inhibitor sodium azide on the uptake of a 3-PLG-dopa and 3-PLG-dopa-A-GSH, and b 3-PLG-ibu and 3-PLG-ibu-A-GSH nanocarriers. Values presented are means  $\pm$  SD and are given as a percentage of the non-targeted nanoparticle groups. Statistical analysis: two-way ANOVA, Dunnett post-test; \* $p < 0.05$ ; \*\*\* $p < 0.001$ ; \*\*\*\* $p < 0.0001$  compared to the non-treated control in each groups; #### $p < 0.0001$  compared to non-targeted groups.  $n = 4-6$  (Mészáros et al., 2025).

The A-GSH dual-targeting also resulted in enhanced permeability across the improved human co-culture BBB model for both drug-coupled nanocarriers (Mészáros et al. 2025).

#### *Effect of dual-targeted and drug-coupled nanocarriers under pathological conditions*

##### *-Ibuprofen-coupled nanocarriers*

The protective effects of ibuprofen-coupled nanocarriers were tested against cytokine-induced damage on the improved human BBB culture model. First, the kinetics and concentration-dependency of cytokine damage was investigated on the human BBB model showing tighter barrier properties. The combination of TNF- $\alpha$  and IL1- $\beta$  cytokines (10 ng/ml each) was effective and caused a 30 % decrease in the impedance of differentiated human brain endothelial cells at the 24-hour time point. Second, we verified the protective effects of the ibuprofen-coupled nanocarriers against cytokines. Treatment with 3-PLG-ibu-A-GSH in the presence of cytokines significantly protected the cells at 24 hours as compared to the cytokine-treated group (20% vs 30% decrease in impedance, respectively) (Mészáros et al. 2025). No protection was seen in the free ibuprofen and 3-PLG-ibu co-treatment groups.

The BBB permeability of ibuprofen-coupled nanocarriers was also tested under pro-inflammatory conditions (Fig. 7A-B; Mészáros et al. 2025). CK-treatment caused significant increase on the permeability of the non-targeted nanocarrier 3-PLG-ibu but it had no influence on the penetration of the targeted 3-PLG-ibu-A-GSH. The targeted nanocarriers showed significantly higher permeability compared to the non-targeted nanoparticles both in control conditions and in the presence of cytokines. The penetration of the small paracellular permeability marker sodium fluorescein (376 Da) and the large transcellular marker Evans-blue albumin complex (67 kDa) were significantly lower in the 3-PLG-ibu-A-GSH and cytokine co-treatment group, compared to the cytokine-treated group, suggesting that 3-PLG-ibu-A-GSH as a drug-coupled targeted nanocarrier is effective against BBB-damage.

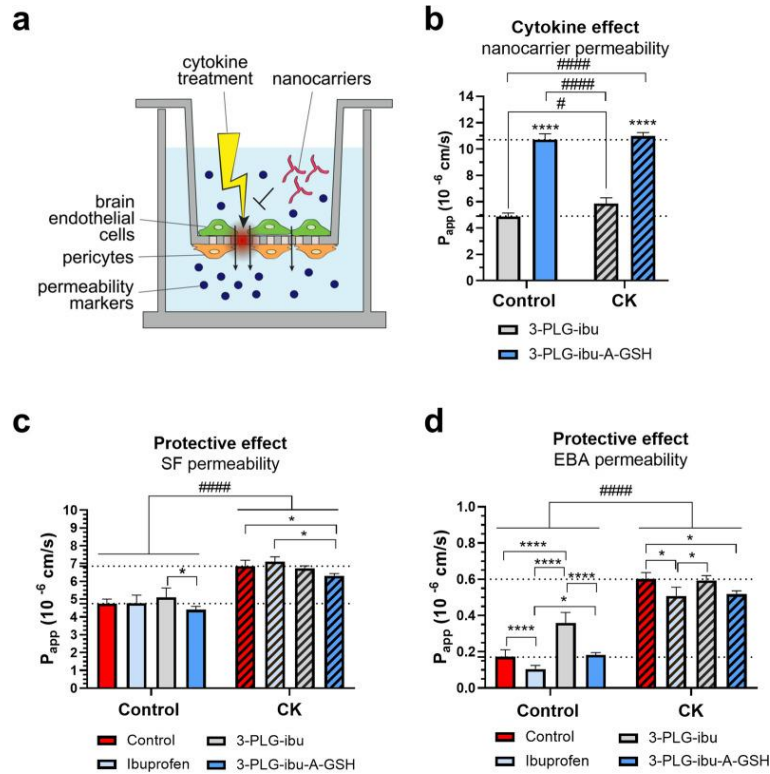


**Fig. 7.** Protective effects of ibuprofen-coupled nanocarriers (3-PLG-ibu and 3-PLG-ibu-A-GSH) and ibuprofen against cytokine-induced (CK) barrier dysfunction in a human BBB co-culture model. *a* schematic drawing of the set-up. *b* Effect of CK on the permeability of 3-PLG-ibu and 3-PLG-ibu-A-GSH nanocarriers across the BBB model. Values presented are means  $\pm$  SD. Statistical analysis: two-way ANOVA followed by Tukey's post-test; comparisons within the treatment groups \*\*\*\* $p < 0.0001$ ; comparisons between the control and the CK groups; # $p < 0.05$ ; #### $p < 0.0001$ ;  $n = 4$ .  $P_{app}$ : apparent permeability coefficient. Penetration of *c* sodium fluorescein (SF) and *d* Evans blue-albumin (EBA) reference marker molecules after a 24-h permeability assay with nanocarriers or free ibuprofen (1.5  $\mu$ M) with or without CK-treatment. Values presented are means  $\pm$  SD. Statistical analysis: two-way ANOVA followed by Tukey's post-test; comparisons within the treatment groups \* $p < 0.05$ ; \*\*\*\* $p < 0.0001$ ; comparisons between the control and the CK groups; #### $p < 0.0001$   $n = 4$ .  $P_{app}$ : apparent permeability coefficient (Mészáros et al., 2025).

#### -Dopamine-coupled nanocarriers

We demonstrated that the targeted 3-PLG-dopa-A-GSH nanocarriers after crossing the BBB could enter at significantly higher concentration into midbrain-like organoids generated from healthy (control) and Parkinson's disease (PD) patient-specific stem cells compared to the untargeted 3-PLG-dopa group both in static (Fig. 8A-C; Mészáros et al., 2025) and microfluidic (manuscript under preparation) improved models of human BBB. Midbrain organoids were provided by the group of our cooperation partner, Prof. Jens Schwamborn, University of Luxembourg. There was no significant difference in the penetration of targeted nanocarriers between the control and the PD organoids neither in the static model nor in the lab-on-a-chip device under flow conditions.

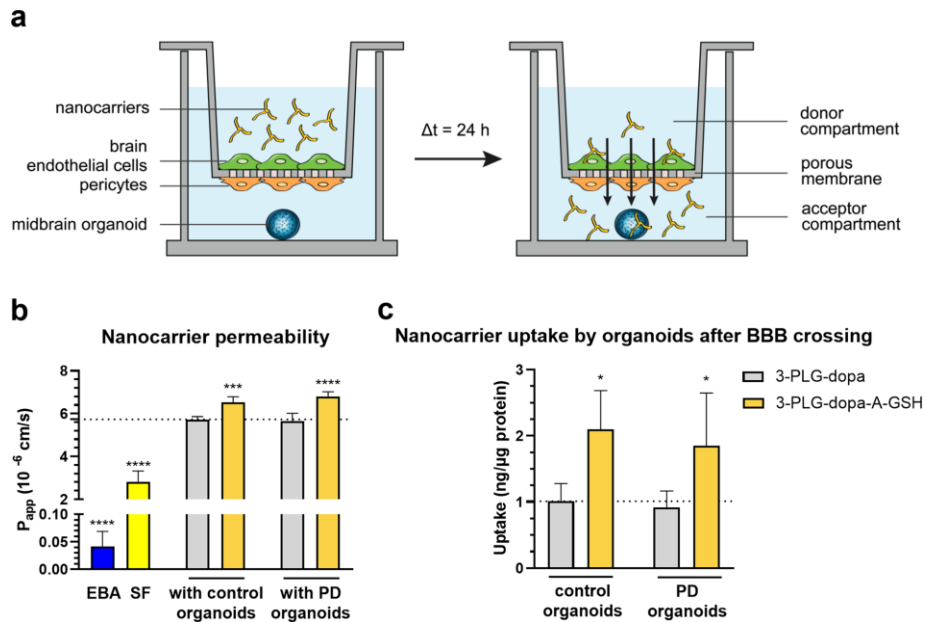


**Fig. 8.** Permeability of non-targeted (3-PLG-dopa) and alanine-glutathione-targeted (3-PLG-dopa-A-GSH) nanocarriers across the human BBB co-culture model and entry into human midbrain-specific organoids. *a* Schematic drawing of the experimental set-up. *b* Permeability of dopamine coupled nanocarriers, and Evans blue-albumin (EBA) and sodium fluorescein (SF) reference marker molecules across the co-culture model in the presence of midbrain-specific organoids derived from healthy (control) and Parkinson's disease (PD) patients' cells. *c* Cellular uptake of nanocarriers by organoids after crossing the BBB. Values are means  $\pm$  SD. Statistical analysis: two-way ANOVA, Tukey's post-test.  $*p < 0.05$ ,  $***p < 0.001$ ,  $****p < 0.0001$  compared to the 3-PLG-dopa data in both organoid groups. Permeability values of EBA and SF were compared to the 3-PLG-dopa group with control organoids ( $****p < 0.0001$ ; one-way ANOVA, Dunnett test).  $n = 6$  organoids/group.  $P_{app}$ : apparent permeability coefficient (Mészáros *et al.*, 2025).

These results corroborate that the BBB-targeted, ibuprofen- or dopamine-coupled poly(L-glutamic acid) polypeptides can be used as nanocarriers for nervous system application. The appropriate combination of the ligands for BBB nutrient transporters (A-GSH) can help brain delivery both under physiological and pathological conditions.

## Summary

Current gold standard culture models of the blood-brain barrier (BBB) used for drug testing are based on primary brain endothelial cells isolated from brain tissues animals. Due to species differences the development of human cell-based models has high importance. We developed an improved and physiologically more relevant human BBB model based on the co-culture of vascular endothelial cells derived from human cord blood stem cells with brain pericytes using novel small molecular differentiation factors. To enhance BBB properties, we activated the cyclic AMP/PKA and Wnt/ $\beta$ -catenin signaling pathways, and inhibited the TGF- $\beta$  pathway. To target this interaction, we developed a small-molecule cocktail named cARLA, which synergistically enhanced barrier properties in a range of BBB models.

We also presented a novel BBB-targeted nanodrug delivery system coupled with dopamine and ibuprofen investigated on the cARLA-improved human BBB model. Targeted nanoformulations of both drugs showed elevated cellular uptake in a time-dependent, active manner via endocytic mechanisms. Addition of free ligands inhibited the cellular internalization of targeted nanocarriers suggesting the crucial role of ligands in the uptake process. A higher permeability across the BBB model was measured for targeted nanocarriers. After crossing the BBB, targeted dopamine nanocarriers subsequently entered midbrain-like organoids derived from healthy and Parkinson's disease patient-specific stem cells. The ibuprofen-coupled

targeted nanocarriers showed protective effects against cytokine-induced barrier damage. In conclusion, the BBB-targeted nanocarriers coupled to therapeutic molecules were effectively taken up by brain organoids or showing a BBB protective effect indicating potential applications in nervous system pathologies.

## References

- Kreuter J. Drug delivery to the central nervous system by polymeric nanoparticles: what do we know? *Adv. Drug. Deliv. Rev.* 2014; 71:2-14.
- McCarthy DJ, Malhotra M, O'Mahony AM, et al. Nanoparticles and the blood-brain barrier: advancing from in-vitro models towards therapeutic significance. *Pharm. Res.* 2015; 32:1161-1185.
- Mészáros M, Porkoláb G, Kiss L, et al. Niosomes decorated with dual ligands targeting brain endothelial transporters increase cargo penetration across the blood-brain barrier. *Eur. J. Pharm. Sci.* 2018; 123:228-240.
- Mészáros M, Phan THM, Vigh JP, Porkoláb G, Kocsis A, Páli EK, Polgár TF, Walter FR, Bolognin S, Schwamborn JC, Jan JS, Deli MA, Veszélka S. Targeting Human Endothelial Cells with Glutathione and Alanine Increases the Crossing of a Polypeptide Nanocarrier through a Blood-Brain Barrier Model and Entry to Human Brain Organoids. *Cells.* 2023 Feb 3;12(3):503.
- Mészáros M, Phan THM, Vigh JP, Porkoláb G, Kocsis A, Szecskó A, Páli EK, Cser NM, Polgár TF, Kecskeméti G, Walter FR, Schwamborn JC, Janáky T, Jan JS, Veszélka S, Deli MA. Alanine and glutathione targeting of dopamine- or ibuprofen-coupled polypeptide nanocarriers increases both crossing and protective effects on a blood-brain barrier model. *Fluids Barriers CNS.* 2025;22(1):18.
- Neuwelt E, Abbott NJ, Abrey L, et al. Strategies to advance translational research into brain barriers. *Lancet Neurol.* 2008; 7:84-96.
- Pardridge WM. CSF, blood-brain barrier, and brain drug delivery. *Expert. Opin. Drug. Deliv.* 2016; 13:963-975.
- Pardridge, W.M. Delivery of biologics across the blood-brain barrier with molecular trojan horse technology. *BioDrugs.* 2017; 31:503-519.
- Porkoláb G, Mészáros M, Szecskó A, Vigh JP, Walter FR, Figueiredo R, Kálmista I, Hoyk Z, Vizsnyiczai G, Gróf I, Jan JS, Gosselet F, Pirity MK, Vastag M, Hudson N, Campbell M, Veszélka S, Deli MA. Synergistic induction of blood-brain barrier properties. *Proc Natl Acad Sci U S A.* 2024;121(21):e2316006121.
- Uchida Y, Yagi Y, Takao M, et al. Comparison of Absolute Protein Abundances of Transporters and Receptors among Blood-Brain Barriers at Different Cerebral Regions and the Blood-Spinal Cord Barrier in Humans and Rats. *Mol. Pharm.* 2020; 17:2006-2020.
- Veszélka S, Mészáros M, Kiss L, et al. Biotin and glutathione targeting of solid nanoparticles to cross human brain endothelial cells. *Curr. Pharm. Des.* 2017; 23:4198-4205.
- Veszélka S, Tóth A, Walter FR, et al. Comparison of a rat primary cell-based blood-brain barrier model with epithelial and brain endothelial cell lines: gene expression and drug transport. *Front. Mol. Neurosci.* 2018; 11:166.